

## **Arrayed ZnO Nanorods Fabrication on ZnO Film by Self-catalyst Growth Method in Aqueous Solution**

E. K.C. Pradeep<sup>1</sup>, X. Li<sup>1</sup>, T. Kawaharamura<sup>1</sup>, D. Wang<sup>2</sup>, A. Hatta<sup>1</sup>, C. Li<sup>1\*</sup>

<sup>1</sup> Institute for Nanotechnology, Kochi University of Technology, Kami city, Kochi 782-8502, JAPAN

<sup>2</sup> Department of Environmental Science and Engineering, Kochi University of Technology, Kami city, Kochi 782-8502, JAPAN

### **ABSTRACT**

ZnO nanorods were grown up from as-deposited ZnO film on which the zinc self-catalysts generated by a novel reducing method. Well aligned ZnO nanorods with a uniform high aspect ratio were grown up on multi-annealed samples. The length of nanorods depended significantly on the reaction time in the hydrothermal synthesis.

### **INTRODUCTION**

ZnO has received a very high attention from different research groups around the world, owing to its chemical, physical, and electrical properties. ZnO is an amphoteric material having a direct wide band gap (3.37 eV), and high exciton binding energy (60 meV), and it can be prepared with a good crystallinity [1,2]. Recently, ZnO nanostructures including nanorods, and nanowires have been widely experimented to be used in dye sensitized solar cells [3], ZnO-polymer hybrid LEDs [4], photo catalysts [5] and piezoelectric generators [6].

Various physical and chemical methods have been used to fabricate one-dimensional arrays of ZnO nanostructures [7-10]. Some of physical methods, such as, chemical vapor deposition [11], pulsed laser deposition [12] and molecular beam epitaxy [13] are less attractive, comparing to chemical methods [8], due to the requirement of high temperature and vacuum processes. Electrodeposition and hydrothermal synthesis are low cost ecofriendly chemical fabrication methods [9,14]. However, the application of electrodeposition method is limited to conductive substrates. Therefore, the hydrothermal synthesis has become one of most popular synthetic methods for one-dimensional ZnO nanostructure fabrication [15].

Most of hydrothermal synthesis methods for ZnO nanostructure fabrication require catalyst assistance [16]. Transition metals are commonly used as catalysts [17,18], and those catalytic seeds contaminate nanostructures [19]. Up to date, there are a few reports for growing-well arrayed ZnO nanostructures with a catalyst free or self-catalyst growth method. In this work, a novel self-catalyst growth hydrothermal method for arrayed ZnO nanorod fabrication is demonstrated. The obtained nanorods were fabricated on a transparent conductive oxide glass substrate are expected to be used as the photo-anodes of dye sensitized solar cells (DSSCs) in future experiments.

### **EXPERIMENTAL DETAILS**

Double layered ZnO films (150nm/25nm) were deposited on Indium-Tin-Oxide (ITO) glass substrates using a conventional 13.56 MHz radio frequency (RF) magnetron sputtering

system. The RF power of the system was 180 W. A 4-inch ZnO (99.999%) ceramic target was located on a cathode 60 mm distance from a substrate stage. The sputtering chamber was evacuated up to about  $6 \times 10^{-5}$  Pa with the aid of a turbo molecular pump. The substrate was preheated to 150 °C for 20 min prior to deposition, and the substrate temperature was maintained during the deposition process. The deposition process of ZnO buffer layer (25 nm) was carried out in a mixture of Ar<sub>(g)</sub> and O<sub>2(g)</sub>. The mass flow rates of Ar<sub>(g)</sub> and O<sub>2(g)</sub> were 30 and 10 (sccm), respectively. The deposition process of ZnO thin film was carried out in Ar<sub>(g)</sub> ambient (30 sccm). For the whole deposition process, the working pressure was maintained at 7 Pa.

Thereafter, the ZnO thin films deposited ITO glass substrates were subjected to a single or multiple reducing annealing process. In single annealing process, samples were annealed in a forming gas ambient (1.9 % H<sub>2(g)</sub> in N<sub>2(g)</sub>). The temperature of the furnace was maintained at 300 °C for 2 hours and then elevated gradually to 400 °C in 5 minutes and then maintained for another 2 hours. In multiple reducing annealing process, the first step of annealing was the same as the single annealing process. In the second step, the ambient was changed to O<sub>2(g)</sub> and samples were maintained in the ambient for 2 hours, then samples were restored in a forming gas again (1.9 % H<sub>2(g)</sub> in N<sub>2(g)</sub>) for 2 hours whilst maintaining the temperature at 400 °C. Prior to each ambient transition step, N<sub>2(g)</sub> was purged through the furnace due to safety reasons.

After annealing, samples were placed in a hydrothermal synthesis bath containing a 12.5 mM aqueous solution of Zn(NO<sub>3</sub>)<sub>2</sub>·6H<sub>2</sub>O and hexamethylenetetramine (C<sub>6</sub>H<sub>12</sub>N<sub>4</sub>, HMTA) at 95 °C. The hydrothermal synthesis procedure was continued for 40 hours, and the solution was replenished after each 4 hours.

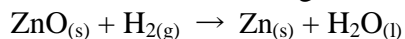
A field emission scanning electron microscope (FE-SEM) system (JEOL-JSM7400F) was used to characterize the surface morphology of ZnO films and ZnO nanostructures. Optical transmittance spectra of ZnO films or ZnO nanostructures deposited on ITO glass substrates were recorded by a (Hitachi U-4100) spectrophotometer. X-ray diffraction patterns of ZnO films and nanorods were recorded by using a Rigaku ATX-G X-ray diffractometer.

## DISCUSSIONS

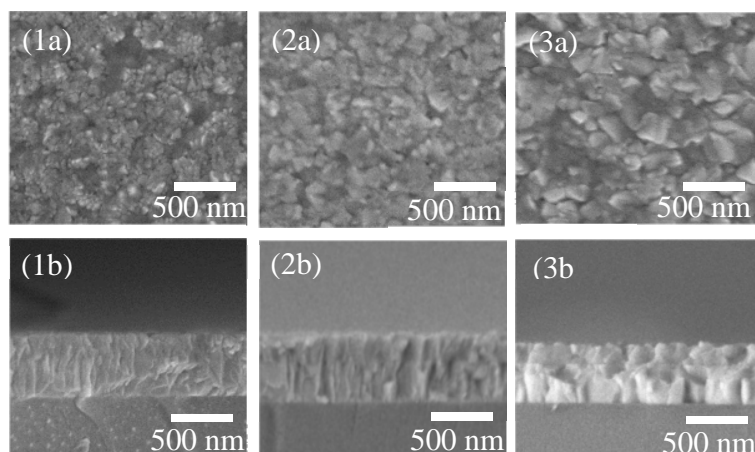
### Zinc self-catalyst preparation

Fig. 1 (1a), (1b) shows the top and cross sectional FE-SEM images of a ZnO film deposited on ITO glass. These FE-SEM images indicate that a uniform ZnO thin film was deposited on ITO glass. Fig. 1(2) and (3) shows the (a) top view and (b) cross sectional FE-SEM images of ZnO films after being subjected to single or multiple reducing annealing process.

In the annealing process, ZnO film reacts with H<sub>2(g)</sub>; the increased temperature promotes the rate of the reaction given below [7].



Zn<sub>(s)</sub> metal nuclei formed by the reducing annealing can serve as the self-catalysts in the hydrothermal synthesis process. In our previous studies, we have found that ZnO nano nuclei could be grown by both single and multiple reducing annealing method [7], and these ZnO nuclei could serve as self-catalysts for ZnO nanorods further grown in a hydrothermal synthesis process. After the reducing-annealing process, the formation of self-catalyst seeds could be examined in the SEM images. In this study, the reducing annealing processes were optimized to generate self-catalyst appropriate to be used for hydrothermal growth method.



**Figure 1** (a) Top view and (b) cross sectional FE-SEM images of (1) as deposited (2) singled annealed (3) multi annealed ZnO films

### Hydrothermal synthesis

In the hydrothermal synthesis process, ZnO nanorods were grown on the annealed ZnO films. Fig. 2 (a), (b) and (c) shows the cross section FE-SEM images and the diameter distribution of single, or multiple reducing-annealed samples after hydrothermal synthesis. ZnO nanorods can be grown up on self-catalyst nuclei generated by either single or multiple reducing-annealed samples. ZnO nanorods obtained from the multiple reducing-annealed samples showed higher uniformity with better alignment and high aspect ratio. This can be attributed to the well aligned nanorods type self-catalyst nuclei [20] generated by the multiple reducing annealing process. However, the uniformity of nanorods in single reducing annealed sample was poor and had not a good alignment. Therefore, the multiple reducing annealed-hydrothermally grown sample is more suitable to be used as the photo anode of DSSCs. Hereafter, all the samples discussed in this manuscript were multi annealed followed by a hydrothermal synthesis process.

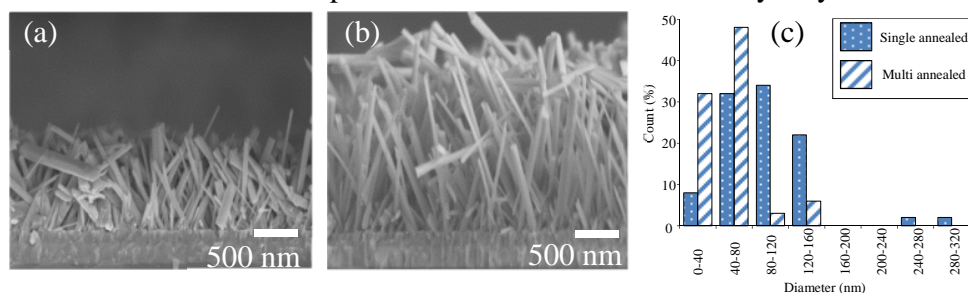


**Figure 2** Cross sectional FE-SEM image of (a) single annealed, (b) multiple annealed samples and (c) diameter distribution of nanorods after hydrothermal deposition

### Nanorods growth: reaction time dependence

Figure 3 shows the chronological growth of ZnO nanorods in the hydrothermal synthesis process. The average length of ZnO nanorods were 125, 650, 1050 and 1550 nm after hydrothermal growth for 4, 8, 12, 16 hours. ZnO nanorods inclined to the substrate were grown on the self-catalyst generated ZnO film with a linear growth rate of about 115 nm/ hour. This

shows that the length of nanorods can be controlled by the reaction time of hydrothermal synthesis.

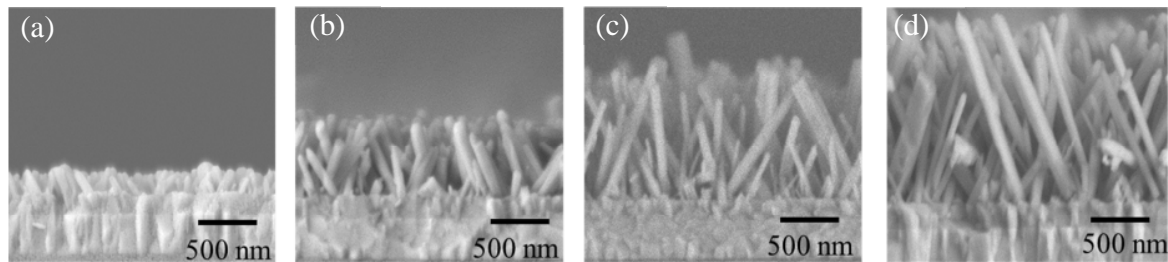


**Figure 3** FE-SEM images of the chronological hydrothermal growth of ZnO nanorods after (a) 4, (b) 8, (c) 12, (d) 16 hours growth times

### **Nanorods growth: parameter optimization for future application**

ZnO nanorods with long length were preferred to increase the anode surface area for the future dye absorption in DSSCs. According to the above experiment, the longer ZnO nanorods, can be obtained easily by increasing the reaction time of hydrothermal synthesis. Figure 4 (a) shows the top view of ZnO nanorods grown up by 20 hours of hydrothermal reaction time. The inserted small image showed the characteristic hexagonal shape of ZnO wurtzite structures [21]. Fig 4 (b) and (c) shows that the average length of ZnO nanorods grown up after 20 and 40 hours reaction time are 2  $\mu\text{m}$  and 3.5  $\mu\text{m}$  respectively.

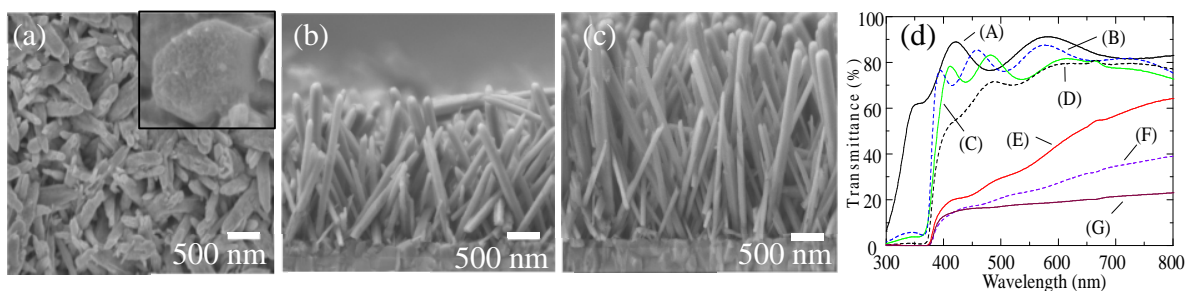


**Figure 4** FE-SEM (a) top view (b) cross sectional images of of 20 hours (c) cross sectional SEM images of 40 hours hydrothermally grown ZnO nanorods (d) optical transmittance spectra of different stages of the process (A) ITO glass, (B) As-deposited (C) multi annealed ZnO film, (D) 4 hours (E) 12 hours (F) 20 hours (G) 40 hours hydrothermally grown samples

Fig. 4 (d) shows optical transmittance spectra at different stages of the process. As the reference, optical transmittance of ITO glass, as-deposited and multi annealed ZnO film were 85 %, 80% and 75% respectively. Optical transmittance were 68%, 40%, 20%, 18% respectively corresponding to the annealed ZnO film grown in 4, 12, 20, 40 hours hydrothermal synthesis method. The optical transmittance was decreased with the hydrothermal reaction time due to the escalated multiple scattering caused by the length increment of the nanorods [22-23]. Comparing to the as-deposited ZnO film, optical transmittance from ZnO nanorods obtained from 20 hours hydrothermal growth had four folds decrement. Optical transmittances of our samples were not as high as preferred transmittance (greater than 75%) for the operation of a DSSC [24]. However, it is possible to improve the optical transmittance of nanorods grown on transparent conductive substrates by controlling the density of nanorods [23]. The further optimized experiment is needed in the future.

Figure 5 shows the X-ray diffraction (XRD) pattern of ZnO nanorods obtained from 20 hours hydrothermal growth. In the XRD pattern peak around  $2\theta = 34.4^\circ$  and  $36.2^\circ$  are corresponding to X-ray diffractions from ZnO wurtzite (002) and (101) planes respectively. Intensity of X-ray diffraction peak corresponding to (101) plane was higher than that of (002) which might be due to the due to the inclined orientation of ZnO nanorods (Fig. 4 (b)) in the sample. These XRD results were well agreed with FE-SEM cross sectional images of ZnO nanorods (Fig. 3 and Fig. 4 (a), (b)).

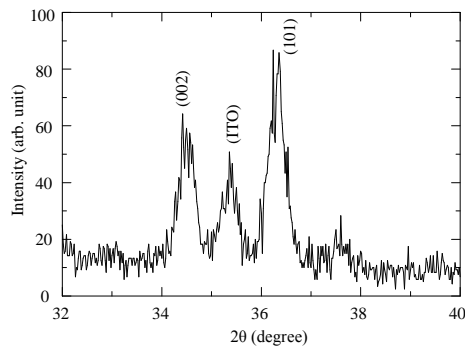
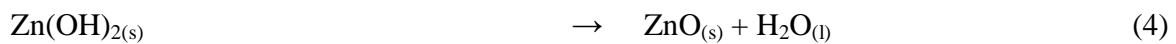
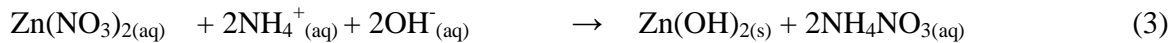
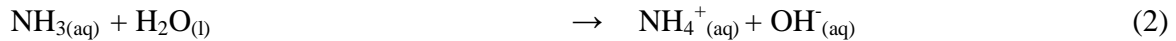
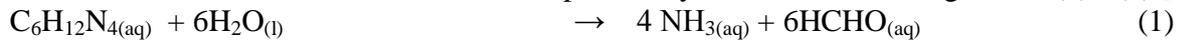


**Figure 5** X-ray diffraction (XRD) pattern of nanorods grown by 20 hours in hydrothermal reaction

### **Growth mechanism**

Growth mechanism of ZnO can be explained by chemical reactions given in (1) - (4) [15].



The hydrolysis of HMTA ( $\text{C}_6\text{H}_{12}\text{N}_4$ ) releases ammonia into the system. The reaction of ammonia and water will increase the concentration of  $\text{OH}^-(\text{aq})$  ions in the solution. This will lead the production of  $\text{Zn}(\text{OH})_2(\text{s})$  by hydroxylation of  $\text{Zn}^{2+}(\text{aq})$  ions. ZnO is produced by the dehydration of  $\text{Zn}(\text{OH})_2(\text{s})$  [17]. It has been reported that the (002) facet of ZnO nanorods are more polar comparing to the (100) surfaces [25]. Hence, when a ZnO nucleus is newly formed, the incoming polar precursor molecules have a higher affinity to polar surfaces. Therefore, the growth rate nanorods, along their own c-axis are higher than that of their a-axis [15, 25]. However, the alignment of initial nuclei and the surface diffusion of precursors in the chemical solution also play an important role for the orientation of nanorods [26]. When the (101) plane of ZnO nanorods was initially grown on (002) axis of ZnO film, ZnO nanorods grow on their own c-axis directed along the length, inclined to ZnO film [27]. This caused to inclined alignment of ZnO nanorods.

### **CONCLUSIONS**

ZnO nanorods were grown up by a self-catalyst assisted hydrothermal synthesis method. Zinc self-catalysts could be generated by reducing annealing of ZnO thin film. Multiple reducing annealing is one of efficient methods to produce well-aligned self-catalyst nuclei which

contribute to the well aligned nanorods. The length of the nanorods increased with the hydrothermal synthesis reaction time.

## ACKNOWLEDGMENT

We gratefully acknowledge the support by Grant-in-Aid for Scientific Research (Grant No: 24561060) from the Ministry of Education, Culture, Sports, Science, and Technology, Japan

## REFERENCES

1. Ü. Özgür, Y. I. Alivov, C. Liu, A. Teke, M. A. Reshchikov, S. Dogan, V. Avrutin, S.-J. Cho, and H. Morkoc, *J. Appl. Phys.* **98**, 041301 (2005)
2. D.C. Look, *Mat. Sci. Eng. B.* **80**, 383 (2001)
3. J. A. Anta, E. Guillén, R.T. Zaera, *J. Phys. Chem. C.* **116**, 11413 (2012)
4. A. Wadeasa, O. Nur, M. Willander, *Nanotechnology.* **20**, 065710 (2009)
5. Q. Wan, T. H. Wang, J. C. Zhao, *Appl. Phys. Lett.* **87**, 083105 (2005)
6. Z.L. Wang, J. Song, *Science* **312**, 242 (2006)
7. C. Li, T. Kawaharamura, T. Matsuda, H. Furuta, T. Hiramatsu, M. Furuta, T. Hirao, *Appl. Phys. Express* **2**, 091601 (2009)
8. W.I. Park, D.H. Kim, S.W. Jung, D.C. Yi, *Appl. Phys. Lett.* **80**, 4232 (2002)
9. D. Pradhan, K.T. Leung, *Langmuir* **24**, 9708 (2008)
10. M.A. Abbasi, Y. Khan, S. Hussain, O. Nur, M. Willander, *Vacuum* **86**, 1998 (2012)
11. J.J. Wu, S.C. Liu, *Adv. Mater.* **14**, 215 (2002)
12. Y. Sun, M. Gareth, M. N. R. Ashfold, *Chem. Phys. Lett.*, **396**, 21 (2004)
13. Y.W. Heo, Y. W. Heo, V. Varadarajan, M. Kaufman, K. Kim, D. P. Norton, F. Ren, and P. H. Fleming, *Appl. Phys. Lett.* **81**, 3046 (2002)
14. H. Zhang, D. Yang, X. Ma, N. Du, J. Wu, D. Que, *J. Phys. Chem. B* **110**, 827 (2006)
15. S. Xu, Z.L. Wang, *Nano Res.* **4**, 1113 (2011)
16. Q. Ahsanulhaq, J. H. Kim, J. H. Kim, Y. Hahn *Nanoscale. Res. Lett.* **5**, 669 (2010)
17. S. H. Jo, J. Y. Lao, Z. F. Ren, R. A. Farrer, T. Baldacchini, J. T. Fourkas, *Appl. Phys. Lett.*, **83**, 4821 (2003)
18. X. XU, M. Wu, M. Asoro, P. J. Ferreira D. L. Fan, *Cryst. Growth Des.* **12**, 4829 (2012)
19. A. Sekar, S.H. Kim, A. Umar, Y.B. Hahn, *J. Cryst. Growth* **277**, 471 (2005)
20. D. Wang, Z. Li, T. Kawaharamura, M. Furuta, T. Narusawa, C. Li, *Phys. Status Solidi C*, **9**, 194 (2012)
21. Z.W. pan, A.R. Dai, Z.L. Wang, *Science* **291**, 1947 (2001)
22. X. Li, C. Pradeep, D. Wang, T. Kawaharamura, N. Nitta, H. Furuta, A. Hatta, C. Li, in *28th European Photovoltaic Solar Energy Conference Exhibition*, Frankreich, France, 2013, pp. 434-436
23. R.T. Zaera, J. Elias, C.L. Clément, *Appl. Phys. Lett.* **93**, 233119 (2008)
24. Y. Chiba, A. Islam, Y. Wathanabe, R. Komiya, N. Koide and L. Han, *Jpn. J. Appl. Phys.*, **45**, 368 (2006)
25. R. A. Laudise, A. A. Ballman, *J. Phys. Chem.* **64**, 688 (1960)
26. J.H. Park, P. Muralidaran, D.K. Kim, *Materials Letters* **63** 1019 (2009)
27. C. Kwak, B. H. Kim, C.I. Park, S. H. Park, S. Y. Seo, S.H. Kim, S.W. Han, *J. Nanosci. Nanotechnol.*, **10**, 912 (2010)